NASA CONTRACTOR REPORT

NASA CR-3

NASA CR-382

A SPECTROSCOPIC METHOD OF TEMPERATURE MEASUREMENT WHICH DOES NOT REQUIRE TRANSITION PROBABILITIES

by R. T. Schneider, W. N. Woerner, and H. E. Wilhelm

Prepared under Contract No. NASw-922 *by*
GENERAL MOTORS
Indianapolis, Ind.
for

NATIONAL AERONAUTICS AND SPACE ADMINISTRATION • WASHINGTON, D. C. • FEBRUARY 1966

NASA CR-382

A SPECTROSCOPIC METHOD OF TEMPERATURE MEASUREMENT WHICH DOES NOT REQUIRE TRANSITION PROBABILITIES

By R. T. Schneider, W. N. Woerner, and H. E. Wilhelm

Prepared under Contract No. NASw-922 by
GENERAL MOTORS
Indianapolis, Ind.

for

NATIONAL AERONAUTICS AND SPACE ADMINISTRATION

For sale by the Clearinghouse for Federal Scientific and Technical Information
Springfield, Virginia 22151 – Price $2.00

A SPECTROSCOPIC METHOD OF TEMPERATURE MEASUREMENT WHICH DOES NOT REQUIRE TRANSITION PROBABILITIES

By R. T. Schneider, W. N. Woerner, and H. E. Wilhelm

SUMMARY

A spectroscopic method is described which allows temperature or pressure measurement without the requirement of knowing the transition probabilities of the spectrum lines employed. Neither calibration of a photographic plate nor use of a radiation standard is required. The measurement is made by comparing the intensity ratios of two spectrum lines emanating from two different locations in the plasma which have different temperatures. The applicability is restricted to those pressure-temperature regions from the point where appreciable ionization starts up to the point of complete ionization. The theory underlying the method is presented and experimental results of applying the method to a cesium plasma are reported.

INTRODUCTION

Most of the spectroscopic temperature measurement methods apply the basic relation for the intensity of spectral lines. Assuming optically thin plasma and Boltzmann distribution of the excited states of the atom, the intensity (I) of a spectral line resulting from a transition $m \rightarrow n$ is given by

$$I_n^m = A_n^m \, g_m \, h\nu_n^m \, \frac{n\,(P,\,T)}{u\,(T)} \, e^{-E_m/kT} \times \ell \qquad (1)$$

where

A_n^m = transition probability

g_m = statistical weight
h = Planck's constant
ν_n^m = frequency
n = $n(P, T)$ = atom density
u = $u(T)$ = partition function
E_m = excitation energy
k = Boltzmann constant
T = temperature, °K
ℓ = geometric length

By means of Equation (1), the temperature can be determined from the experimentally observed absolute line intensity when the transition probability and the atom density are known. However, this requires knowledge of the transition probabilities and also requires an absolute measurement of the radiation power. The requirement for an absolute measurement can be avoided by determining the temperature from the intensity ratio of different spectral lines.[1] * For the transition $m \rightarrow n$ and $p \rightarrow q$, this intensity ratio is given by:

$$\frac{I_n^m}{I_q^p} = \frac{A_n^m g_m}{A_q^p g_p} \cdot \frac{\nu_n^m}{\nu_q^p} \left[e^{-(E_m - E_p)/kT} \right] \tag{2}$$

In this case, only a relative measurement is necessary. Furthermore, only relative transition probabilities must be known for which, in general, more accurate values are available than for absolute transition probabilities.

Relative temperature measurement is possible, finally, without knowledge of transition probabilities.[2,3] This method uses the relation for the intensity ratio of an individual spectral line at different temperatures:

$$\frac{I_n^m(T_1)}{I_n^m(T_2)} = \frac{n(P_1, T_1)\, u(T_2)}{n(P_2, T_2)\, u(T_1)} \; e^{-\left[\frac{E_m}{k}\left(\frac{1}{T_1} - \frac{1}{T_2}\right)\right]} \tag{3}$$

*Superscripts identify references listed at the end of this report.

Equation (3) allows measurement of relative spatial temperature changes and absolute measurement of temperature profiles, if the temperature is already known at one point. If photographic detection is used, the wavelength dependence of the sensitivity of the photographic emulsion need not be known because only intensities of the same wavelength are compared.

If the intensity of a spectral line is plotted versus temperature, then the intensity shows a maximum at a certain temperature. The temperature corresponding to this maximum of radiation intensity can be calculated by the method of Fowler and Milne[4] and used as a reference temperature in Equation (3). Larenz[5] and Bartels[6] employed this method to determine absolute temperature profiles in arcs.

In the following paragraphs, a similar method is described. However, this method does not depend on the observation of an intensity maximum. Also, it does not require knowledge of the transition probabilities or calibration of photographic plates.

METHOD

The derivation of the fundamental relations on which the new method is based is carried through for a plasma consisting of electrons and one kind of ions and neutrals within a temperature range which eliminates considerations of double and higher multiple ionizations. The plasma is presumed to have uniform pressure and to be in approximate local thermodynamic equilibrium.* It should be noted that the assumptions made place no restriction on the method which can readily be extended to plasma mixtures,[7,8] plasmas with nonuniform pressure, and plasmas deviating from thermodynamic equilibrium.

*This elementary plasma model is chosen to demonstrate the principle of the method without too many formal mathematical complications.

Introducing "n_-," "n_+," and "n" as designations for the density of the electrons, ions, and neutrals, respectively, the ionization equilibrium of the plasma is described by Saha's equation:

$$\frac{n_- n_+}{n} = \Phi, \Phi \equiv 2\left(\frac{2\pi m_e}{h^2}\right)^{3/2} \frac{u_+(T)}{u(T)} (kT)^{3/2} e^{-W/kT} \tag{4}$$

where

W = effective ionization energy

$u = \sum_{s=0}^{\infty} g_s e^{-E_s/kT}$ = partition function of the neutrals

$u_+ = \sum_{s=0}^{\infty} g_s^+ e^{-E_s^+/kT}$ = partition function of the ions

g_s, g_s^+ = statistical weights of the intrinsic states of the neutrals and ions

m_e = electron mass

E_s, E_s^+ = excitation energies of the intrinsic states of the neutrals and ions

Equation (4) must be supplemented by the equation of state

$$P = (n_- + n_+ + n)\, kT \tag{5}$$

(equal temperature of the components is assumed) and the condition for electrical neutrality

$$n_- = n_+ \tag{6}$$

From Equations (4), (5), and (6), the particle densities can be calculated as a function of temperature, "T," and total pressure, "P." For the neutral density,

$$n = 2\left[\frac{P}{2\,kT} + \Phi\left(1 - \sqrt{1 + \frac{P}{\Phi kT}}\right)\right] \tag{7}$$

and for the density of the charged particles,

$$n_{\pm} = -\Phi\left(1 - \sqrt{1 + \frac{P}{kT}}\right) \tag{8}$$

Consider now two points in the plasma with different temperatures, T_1 and T_2. Related to these two points, the following fundamental expression can be calculated by means of Equation (7) as a function of temperature T_1

$$b = \log\left[\frac{n(T_1)}{n(T_2)} \cdot \frac{u(T_2)}{u(T_1)}\right], \quad T_2 \cong \frac{T_1}{1 - a\,T_1} \tag{9}$$

where the temperature T_2 has been replaced by introducing the temperature parameter

$$a = \frac{1}{T_1} - \frac{1}{T_2} \tag{10}$$

The expression "b" and the parameter "a" can be measured by spectroscopic methods, as shown in detail in subsequent paragraphs. Thus, by inserting the experimentally determined a-value and b-value into the basic Equation (9), an implicit equation in the temperature T_1 is obtained. From this equation, the temperature T_1 [and because of Equation (10), also the temperature T_2] can be calculated numerically when the pressure is known.

Equation (15) can also be used as the basic relation for absolute measurement of the plasma pressure P. After inserting the experimentally determined a- and b-values, again an implicit relation in T_1 and P is obtained from which the pressure P can be calculated when the temperature T_1 is known. *

---

*Under conditions of different plasma pressures, $P_1 \neq P_2$, only a relative pressure measurement is possible.[8]

In deriving the basic relations for spectroscopic determination of the expression "b" and the parameter "a," the applicability of Boltzmann equilibrium statistics is presumed. The number density of atoms in excited state "m" is then given by**

$$n_m = n(T) \frac{g_m \, e^{-E_m/kT}}{\sum_{s=0}^{\infty} g_s \, e^{-E_s/kT}} \tag{11}$$

For the ratio of the number densities of excited atoms in the state "m" at two different points (T_1) and (T_2), it follows that:

$$\frac{n_m(T_1)}{n_m(T_2)} = \frac{n(T_1)}{n(T_2)} \cdot \frac{u(T_2)}{u(T_1)} \, e^{-\frac{E_m}{k}\left(\frac{1}{T_1} - \frac{1}{T_2}\right)} \tag{12}$$

According to Equations (1) and (12), the intensity ratio of two spectral lines measured at two points with different temperatures (T_1 and T_2) in the same plasma, and resulting from one and the same transition, $m \rightarrow n$, is given by

$$\frac{I_n^m(T_1)}{I_n^m(T_2)} = \frac{n(T_1)}{n(T_2)} \cdot \frac{u(T_2)}{u(T_1)} \, e^{-\frac{E_m}{k}\left(\frac{1}{T_1} - \frac{1}{T_2}\right)} \tag{13}$$

Dividing Equation (13) by the corresponding equation for another transition $p \rightarrow q$, the following relation is obtained:

$$\frac{I_n^m(T_1)}{I_n^m(T_2)} \left[\frac{I_q^p(T_1)}{I_q^p(T_2)}\right]^{-1} = e^{-\frac{(E_m - E_p)}{k}\left(\frac{1}{T_1} - \frac{1}{T_2}\right)} \tag{14}$$

**In the following equations, the dependence on the spatially constant pressure (P) is not indicated for reasons of convenience.

By introducing the temperature parameter "a"—see Equation (10)—and the decadic logarithms of the intensity ratios

$$\Delta Y_n^m = \log \frac{I_n^m (T_1)}{I_n^m (T_2)}$$

$$\Delta Y_q^p = \log \frac{I_q^p (T_1)}{I_q^p (T_2)} \qquad (15)$$

Equation (14) can be rewritten in the form

$$a = \frac{k \ln 10}{E_p - E_m} \left[\Delta Y_n^m - \Delta Y_q^p \right] \qquad (16)$$

This relation permits the temperature parameter "a" to be determined spectroscopically by measuring the decadic logarithms of the intensity ratios defined in Equation (15) for two spectrum lines, $m \rightarrow n$ and $p \rightarrow q$. Similarly, by introducing the fundamental expression "b"—see Equation (9)—Equation (13) can be rewritten in the form:

$$b = \Delta Y_n^m + \frac{E_m}{k \ln 10} \cdot a \qquad (17)$$

This relation shows, finally, that the fundamental expression "b" can be determined experimentally from the measured ΔY_n^m-value and the a-value.

The described method is effective even though the transition probabilities may not be known. According to Equations (16) and (17), only the two excitation energies, E_m and E_p, must be known. The terms ΔY_n^m and ΔY_q^p compare intensities at the same wavelength; therefore, the dependence of sensitivity on the wavelength need not be known. Uncertainties in the spectral sensitivity enter noticeably into the other spectroscopic methods—in particular, the line ratio technique—see Equation (2). It is, therefore, very desirable to remove this source of error.

In Figure 1 the attempt is made to explain the physical meaning of the ΔY and to illustrate how the method works. In this figure, two typical curves—log I versus temperature, T—are plotted. Where I is calculated according to Equation (1), ΔY_n^m and ΔY_q^p are defined by Equation (15) as the logarithm of the ratio of the observed intensities. Since Figure 1 is a logarithm plot of the intensity, ΔY_n^m is represented as the length $\overline{AB} - \overline{CD} = \overline{EB}$. The line $\overline{AB}$ is the logarithm of the intensity observed at the temperature T_1, and $\overline{CD}$ the logarithm of the intensity observed at the temperature T_2. In the same way ΔY_q^p is represented by the length $\overline{AF} - \overline{CH} = \overline{GH}$. If the method is used for temperature determination, ΔY_n^m and ΔY_q^p are measured. To show that it is possible, in a unique way, to derive the temperatures T_1 and T_2 from these measured data, it must first be shown that only one pair of temperatures T_1 and T_2 exists which matches the measured intensities ΔY_n^m and ΔY_q^p.

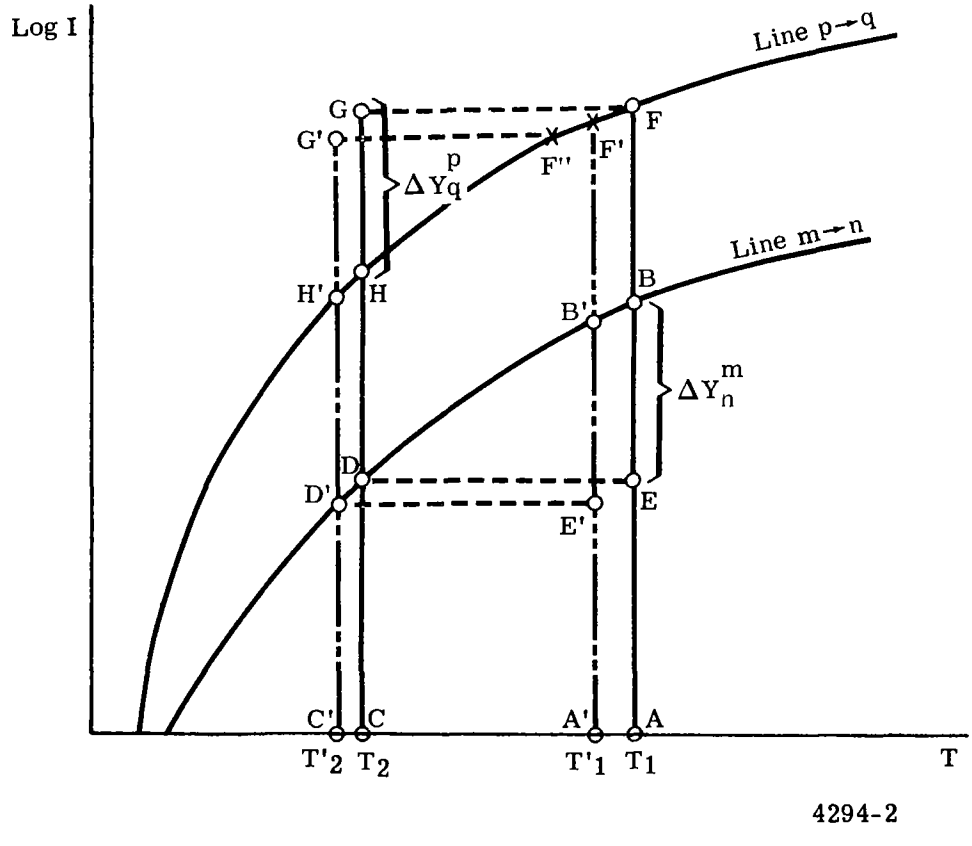

Figure 1. Schematic plot of Log I versus temperature explaining the meaning of ΔY.

Assume the existence of a temperature T_1' which is supposed to match the intensity pairs. Then, since ΔY_n^m is given as a certain length, a second temperature T_2' is automatically defined. $\Delta Y_n^m = \overline{BE} = \overline{B'E'}$. The definition of ΔY_n^m gives $\overline{A'B'} - \overline{C'D'} = \overline{B'E'} = \Delta Y_n^m$.

Since T_2' is now established, $Y_q^p = \overline{GH}$ should be equal to $\overline{G'H'}$ because that is a measured value. If $\overline{G'H'}$ is drawn into the diagram as equal to $\overline{GH}$, the curve of the line $p \rightarrow q$ is not intersected in F' but in F''. This is an inconsistency because ΔY_q^p should be equal to A'F' - C'H' per definition. Therefore only one pair of temperatures ($T_2 T_1$) exists which matches the measured pair of ΔY-values. In this connection, it is remembered that the log I curves of the two different spectrum lines can never be parallel.

It can also now be seen why, in obtaining temperature or pressure measurements, neither the transition probabilities nor a sensitivity calibration of the photographic plate is required. Each would be a constant factor in the equations under consideration. In the log I plot, this would mean a shift of the curve parallel to the log I-axis. It would only change the distances $\overline{BF}$ and $\overline{DH}$. However, neither of them is used in this method.

EVALUATION PROCEDURES

The general mathematical procedure of evaluating the unknown temperature consists of inserting the experimentally observed a- and b-values into Equation (9) and calculating the unknown observable by iteration. In practical situations, however, a graphical presentation aids clarification. For this purpose, the theoretical curves representing the basic expression

$$b = \log \left[\frac{n\,(P,\, T_1) \cdot u \left(\dfrac{T_1}{1 - a\,T_1} \right)}{n \left(P,\, \dfrac{T_1}{1 - a\,T_1} \right) \cdot u\,(T_1)} \right] \qquad (18)$$

are drawn (abscissa) as a function of T_1 wherein "a" and "P" are treated as parameters. From these parametric curve representations, the unknown temperature, T_1, is read as follows. The experimental a-value and the second parameter, P, designate the theoretical b-curve that applies. The experimental b-value gives a definite point on this curve. The ordinate of this point represents the unknown observable.

Theoretical b-curves after Equation (18) for Cs plasmas and a He-Cs mixture are presented in Figures 2 through 10 as convenient for temperature measurement. The graphs can also be used for approximate pressure determination. The used values of pressure, P, seeding ratio, α, and parameter, a, are indicated on the individual graphs.

The ionization potential of Cs is taken as;

$$W_{Cs} = 3.893 \text{ eV}$$

The depression of the ionization potential due to the electrostatic microfield and the Debye-polarization,[9]

$$\Delta W = 0.67 \times 10^{-6} n_-^{1/3} + 0.37 \times 10^{-7} \left(\frac{n_-}{T}\right)^{1/2} \text{ eV} \qquad (19)$$

representing under the given conditions a small correction, was considered by means of a successive approximation.

As an example, consider the Cs lines $8^2 D_{3/2} \rightarrow 6^2 P_{1/2}$ and $6^2 D_{3/2} \rightarrow 6^2 P_{1/2}$, from which the following a- and b-values were observed at a pressure of $P = 10$ dyn cm^{-2}:

$$a = (0.40 \pm 0.06) \times 10^{-4} {}^\circ K^{-1}$$
$$b = 0.25 \pm 0.10$$

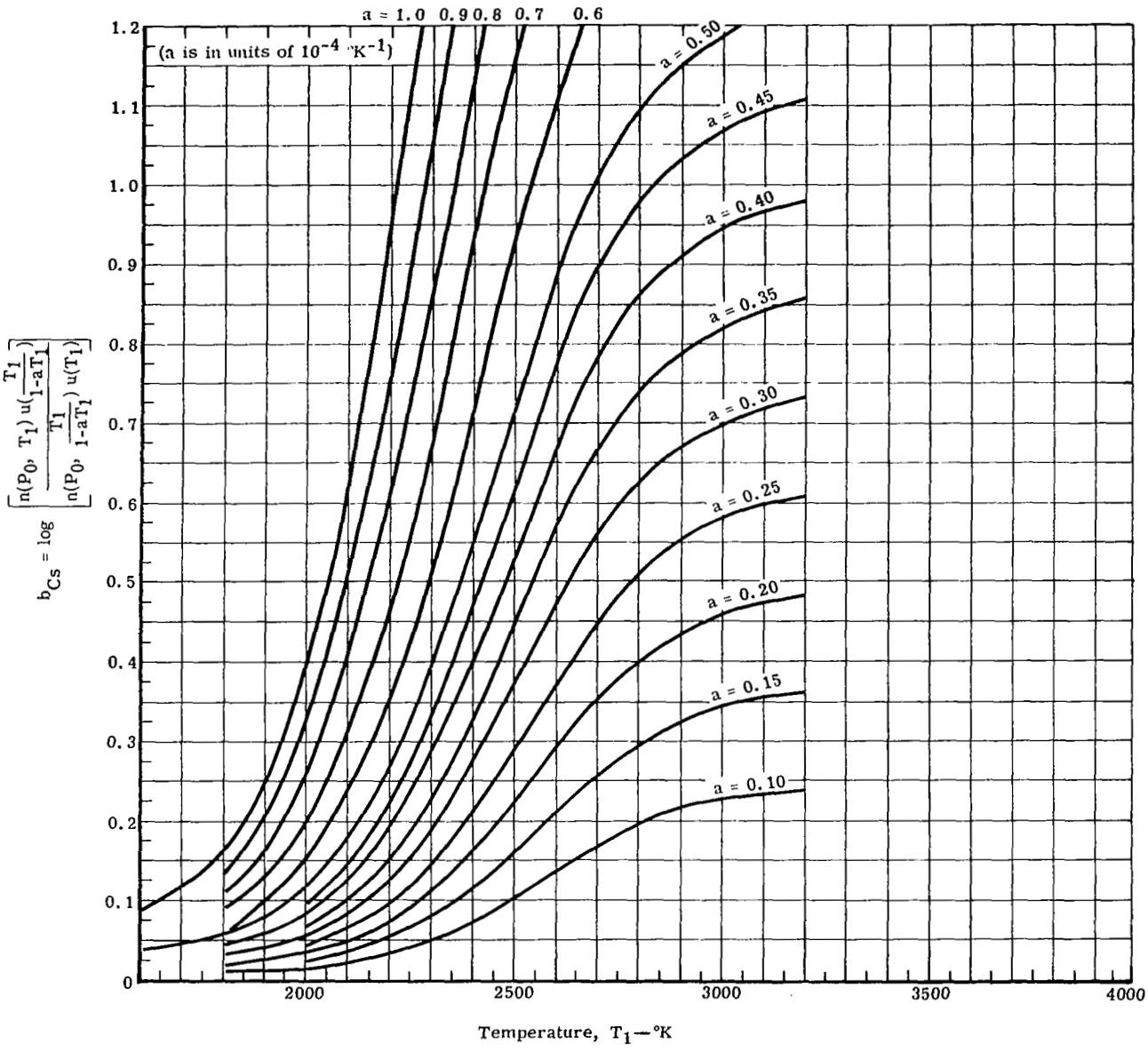

Figure 2. Theoretical b-curves for atomic Cs lines. Pressure: P = 10 dynes/cm^2.

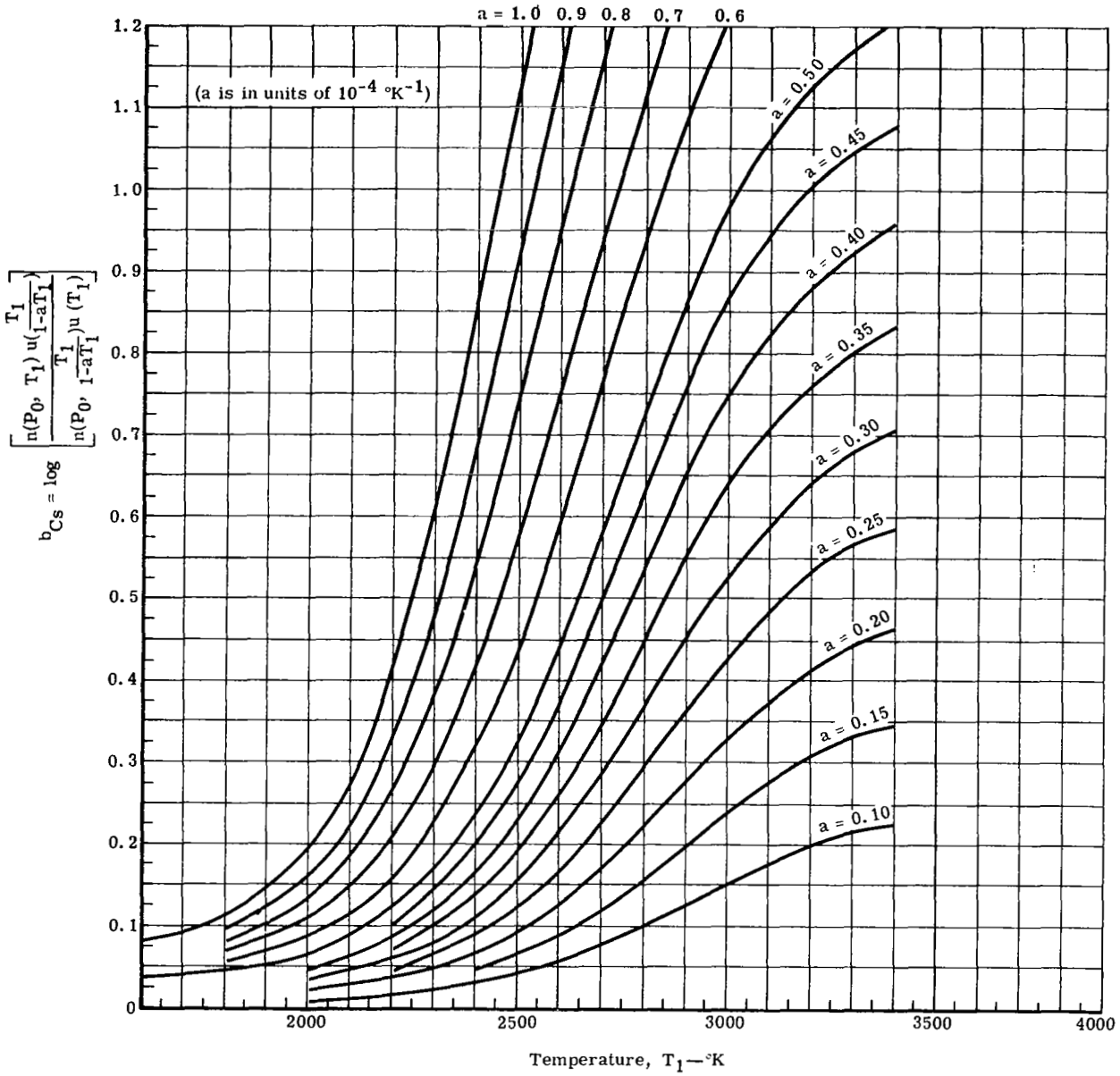

Figure 3. Theoretical b-curves for atomic Cs lines. Pressure: P = 100 dynes/cm^2.

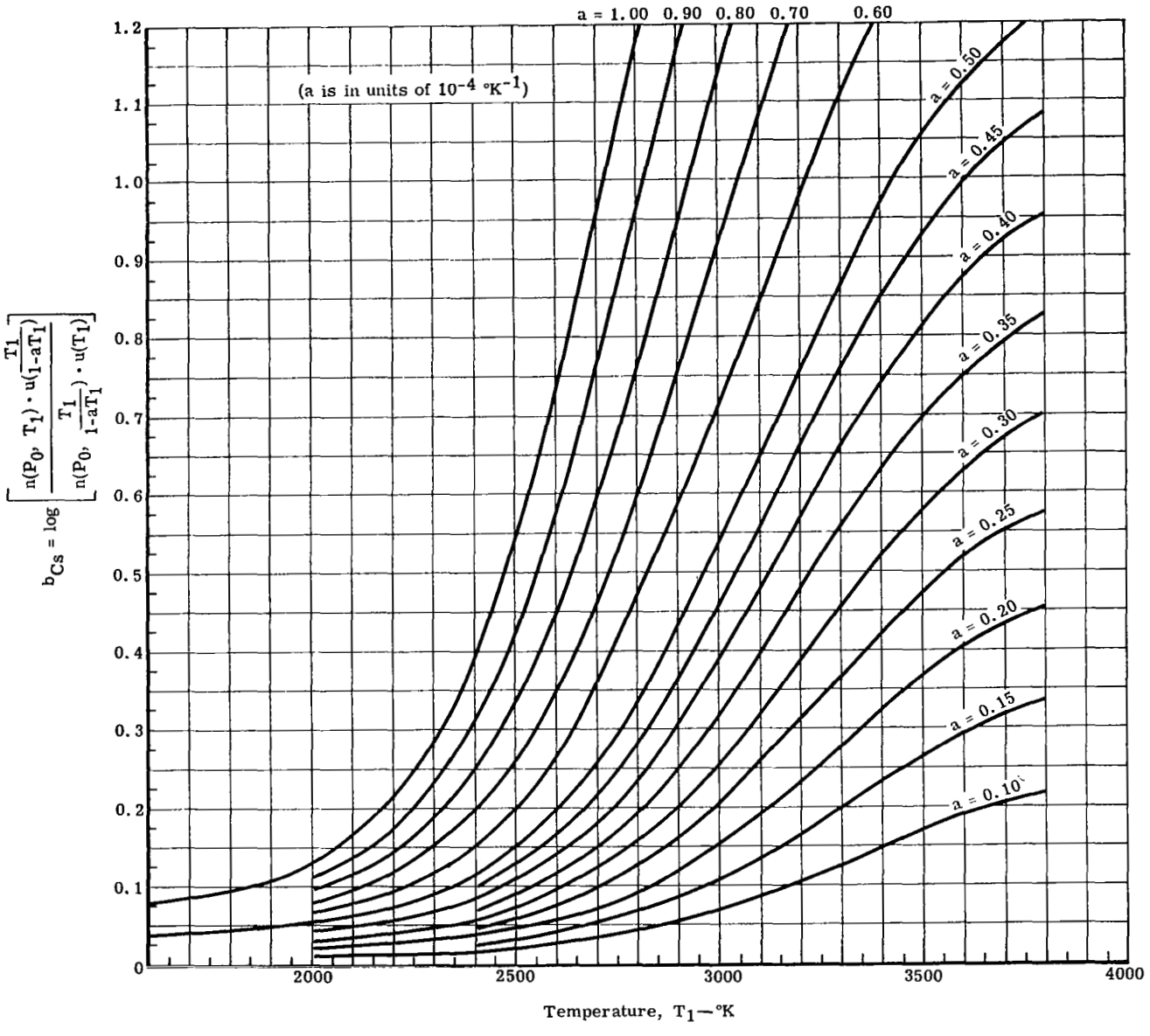

Figure 4. Theoretical b-curves for atomic Cs lines.
Pressure: P = 1000 dynes/cm^2.

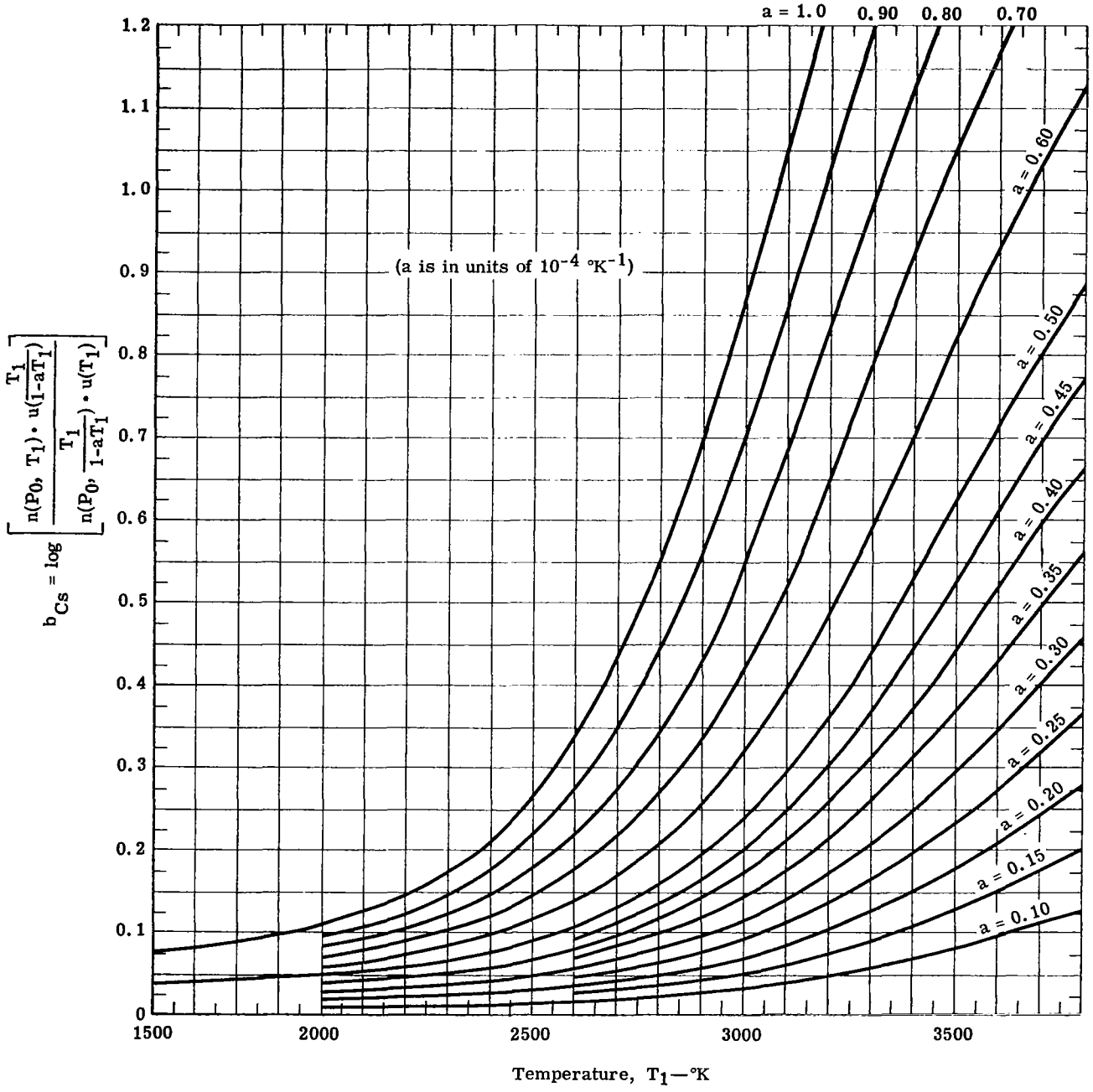

Figure 5. Theoretical b-curves for atomic Cs lines.
Pressure: P = 10,000 dynes/cm^2.

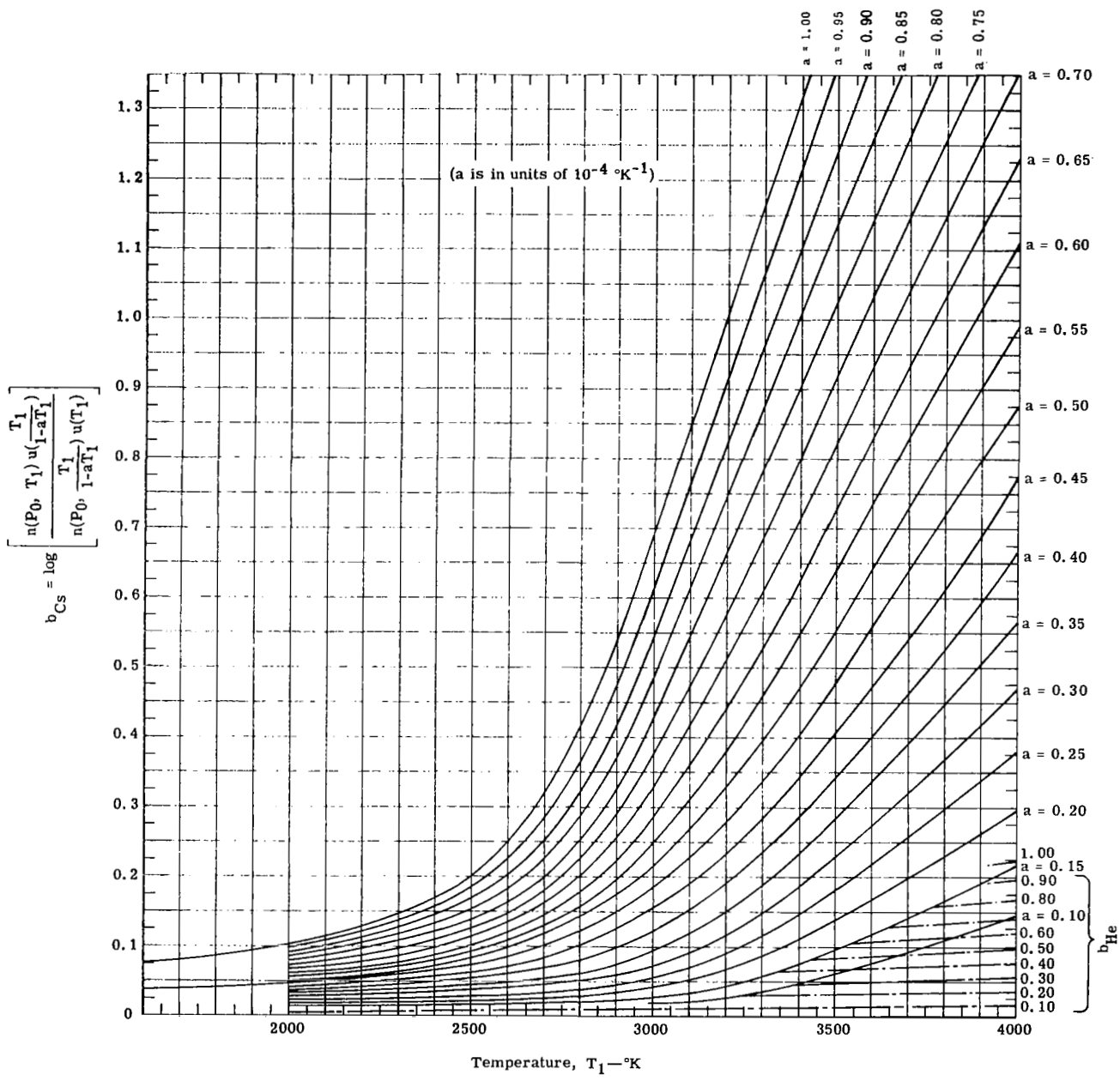

Figure 6. Theoretical b-curves for atomic Cs lines in a He-Cs plasma ($a = 10^{-2}$). Pressure = 1 atm (part 1).

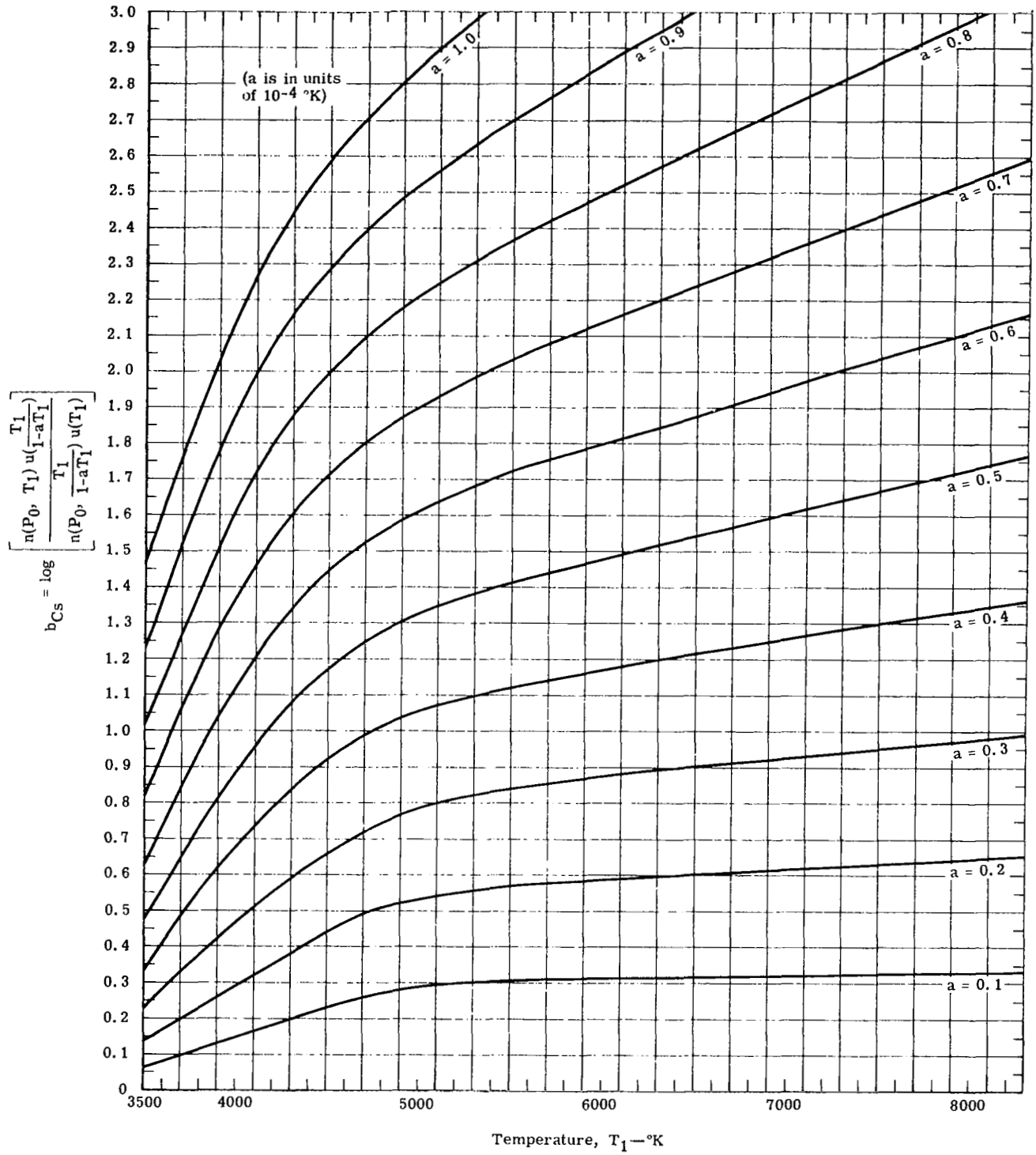

Figure 7. Theoretical b-curves for atomic Cs lines in a He-Cs plasma ($a = 10^{-2}$). Pressure = 1 atm (part 2).

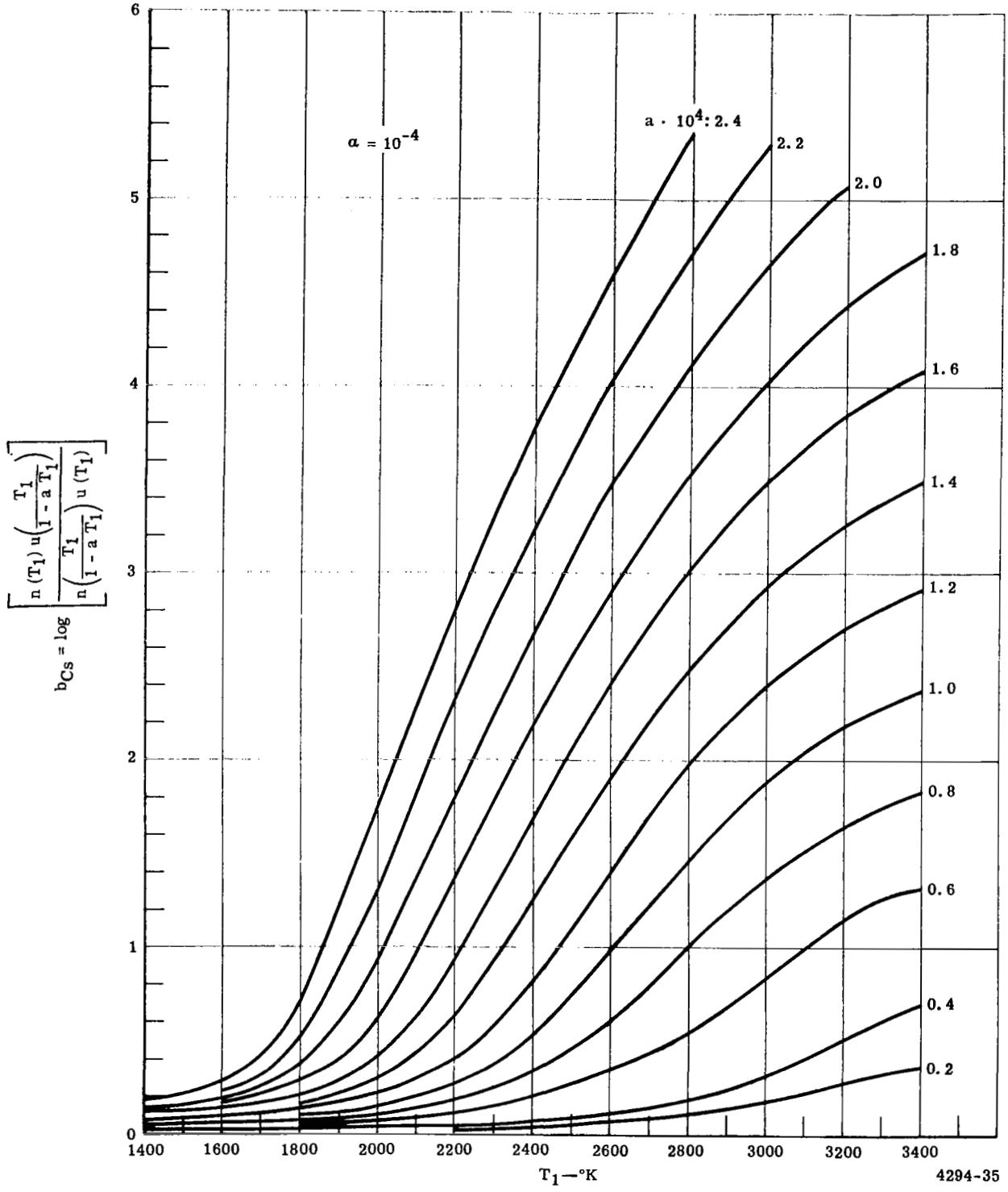

Figure 8. Theoretical b-curves for atomic Cs lines in a He-Cs plasma ($a = 10^{-4}$). Pressure = 1 atm.

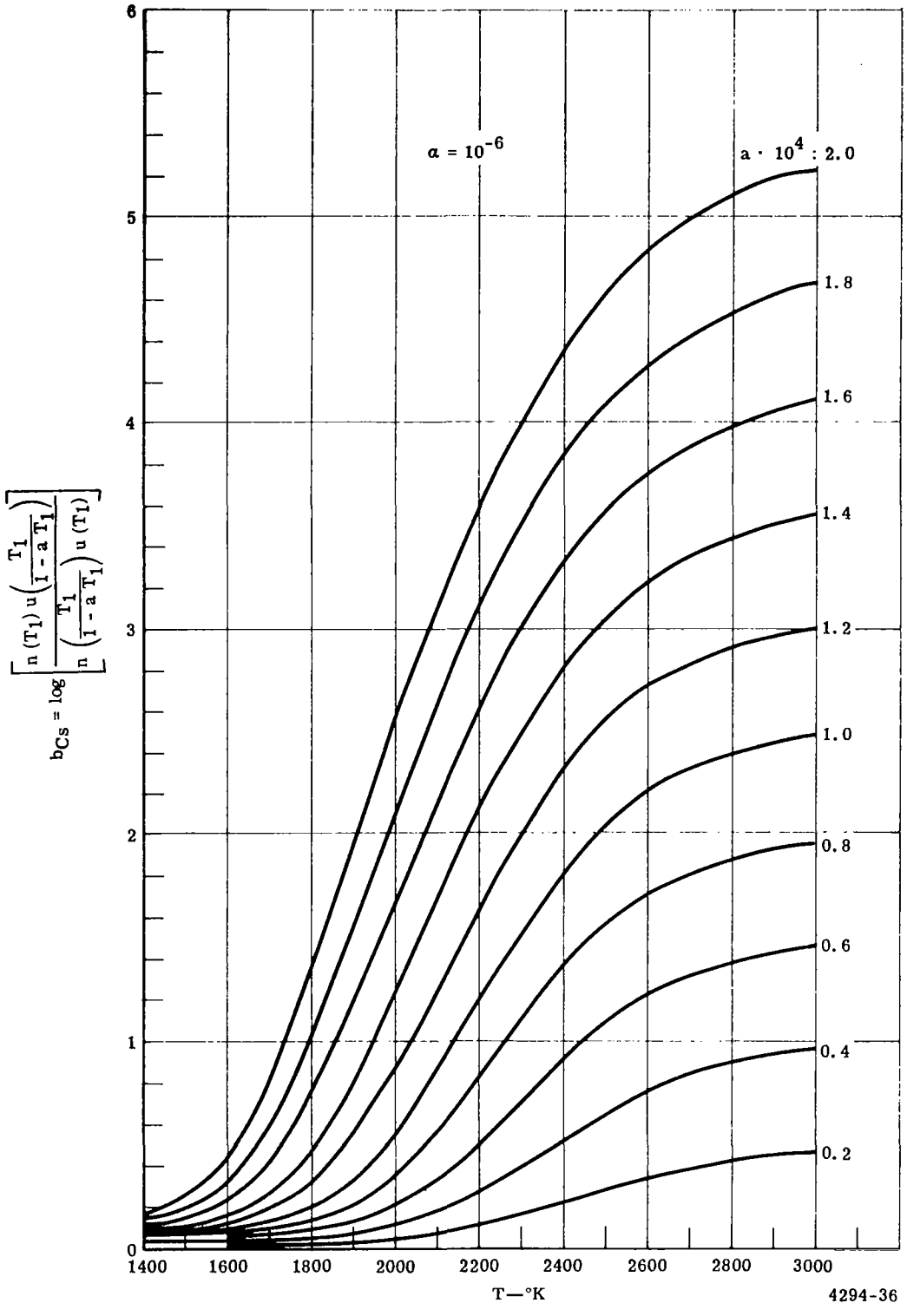

Figure 9. Theoretical b-curves for atomic Cs lines in a He-Cs plasma ($a = 10^{-6}$). Pressure = 1 atm.

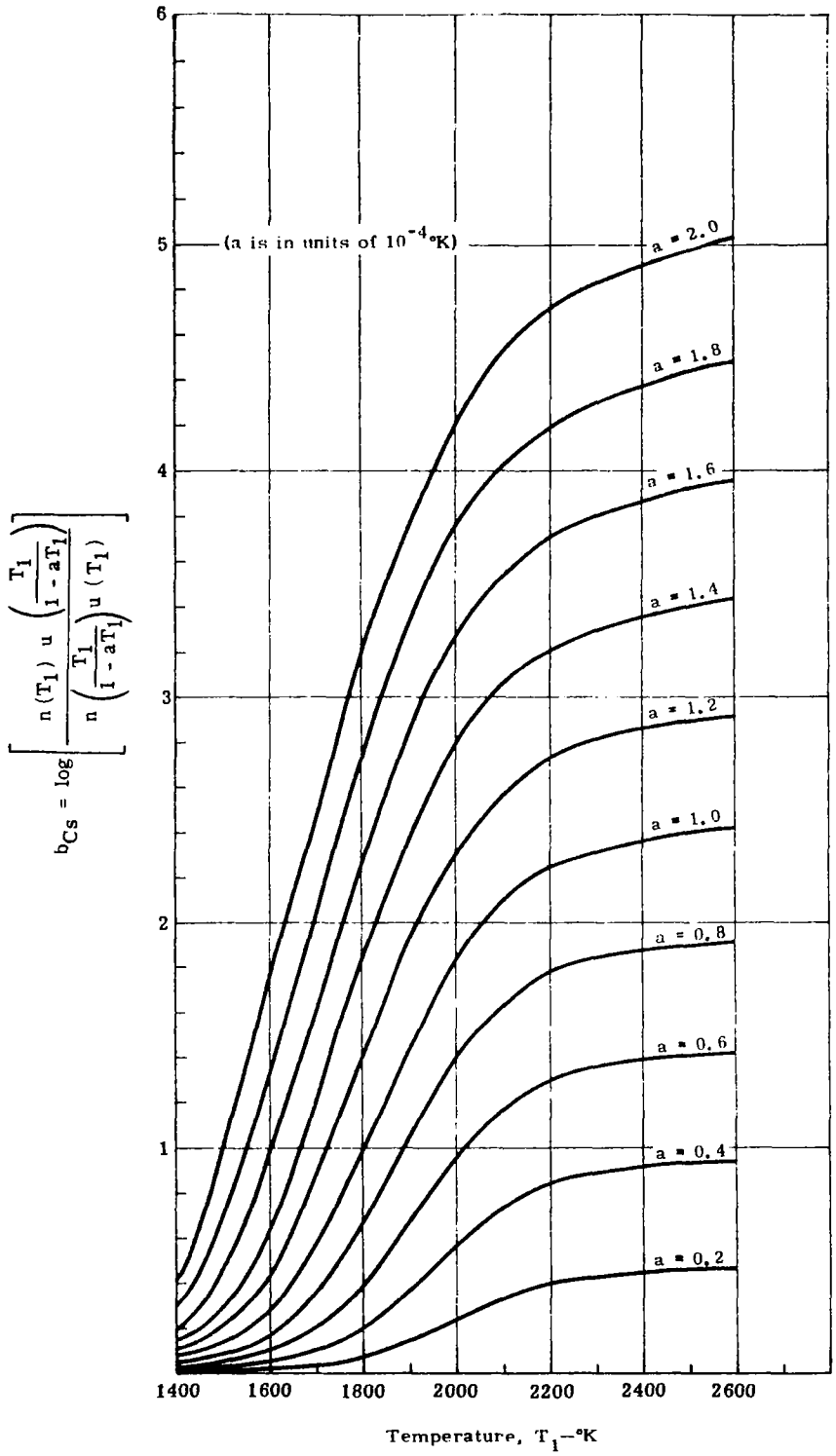

Figure 10. Theoretical b-curves for atomic Cs lines in a He-Cs plasma ($a = 10^{-8}$). Pressure = 1 atm.

Applying these values to the proper curve (see Figure 2), the following is obtained as temperature:

$$T_1 = 2270 \pm 130°K$$

The graphically estimated error (neglecting the influence of the pressure uncertainty ΔP) corresponds to $\frac{\Delta T_1}{T} 100 = 5.6\%$.

EXPERIMENTAL SETUP

To demonstrate the application of the new method on a plasma, a flow stabilized free burning arc was chosen.

Figure 11 shows the schematic of the flow stabilized arc. The gas (in this case, a He-Cs mixture) enters the arc column through a nozzle, surrounding the tungsten cathode. The anode has a center hole through which the heated gas mixture flows. After cooling, it enters a pump and is pumped back into the nozzle. This arc configuration has several advantages. Cathode and anode spots do not jump. The arc column is surrounded by a relatively cold annular flow which stabilizes the arc. The gas stream pulls the cathode spot toward the tip of the tungsten cathode and keeps it fixed there. The anode spot is pulled through the bore in the anode so that this end of the arc also is geometrically fixed. Since the arc column itself can be stabilized with the resulting axial symmetric bell-shaped gas stream between cathode and anode, this configuration seems to be adequate for experiments with Cs-seeded arcs. The gas is heated when leaving by conduction and radiation from the hot cathode (~1800°K) gradually up to about 1000°K before entering the discharge volume. In the arc, the temperature increases up to 4000 to 10,000°K, depending on arc current, seeding ratio, and mass flow. Each of these parameters can be adjusted separately. This adjustability makes it possible to work in almost any desired temperature range.

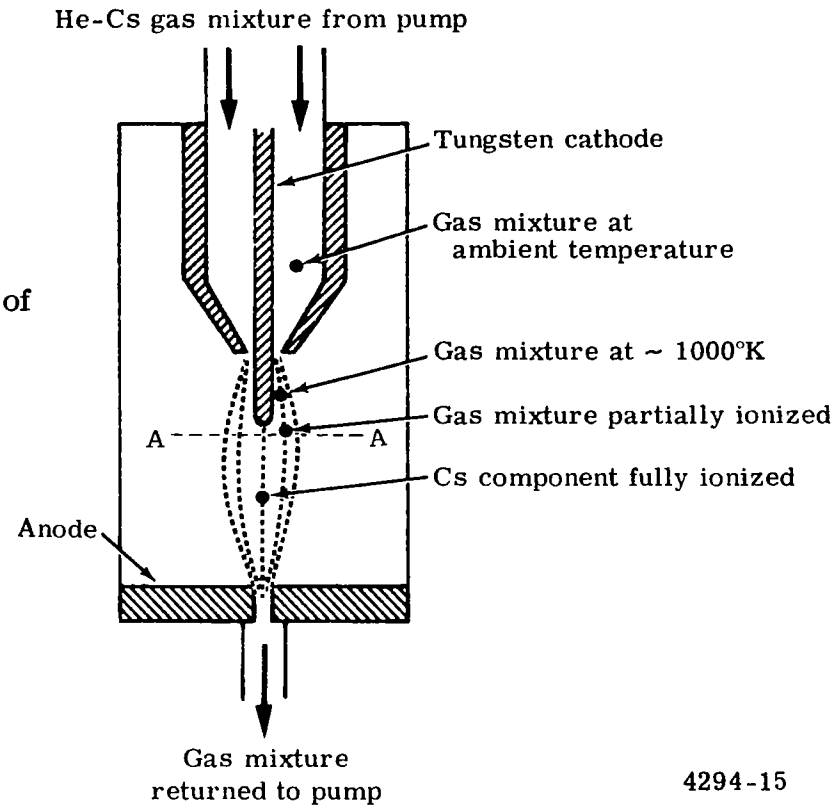

Figure 11. Schematic of flow stabilized arc.

Figure 12 shows the arc assembly. The sapphire observation ports and the electrode assemblies (2) and (3) are flanged on the cylindrical stainless steel chamber.

The anode (2) is a tungsten disk with a 1-mm bore, inserted in a bored solid copper cylinder. The shoulder of the copper cylinder serves as gasket for the knife edges of the vacuum flanges. The copper cylinder is brazed to the water-cooled copper disk. The cathode (3) is a 2.2-mm dia thoriated tungsten rod held by an electrode holder which is brazed to a 0.375-in. copper tube. The copper tube is welded at the tube fitting to the copper gasket between the bellows and the insulator. The insulator provides the cathode with insulation from the stainless steel housing which is filled with the cover gas and encloses the whole assembly. The cathode is insulated from the arc chamber by an insulator. The two stainless steel bellows provide mobility of the cathode relative to arc chamber and housing. The cathode can be moved coaxially about 2 cm, allowing ignition of the arc by contact of cathode and

anode. The seeded gas enters the cathode assembly through the stainless steel tubing and is picked up by a tube. The gas then enters the arc chamber coaxially around the cathode rod (3) and exits through the bore in the anode (2) and stainless steel tube. The stainless steel tubes connect the assembly to the loop.

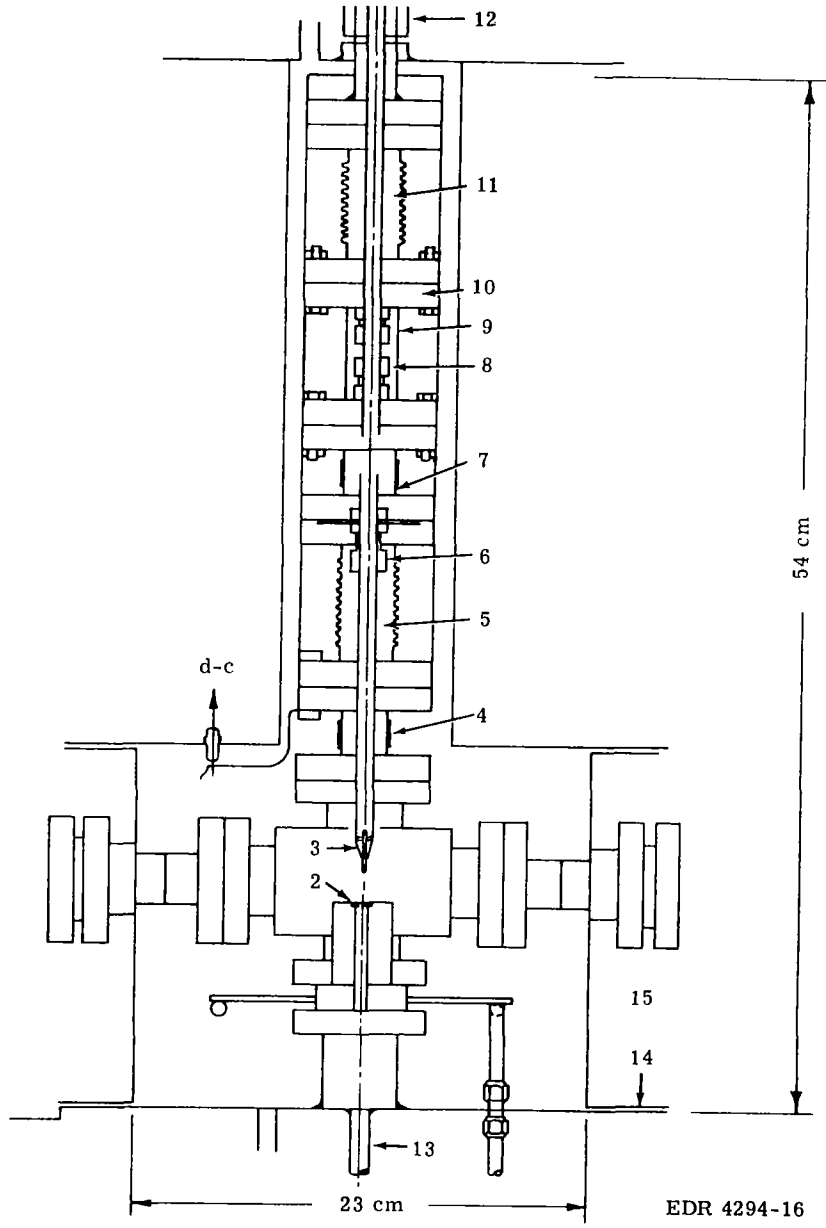

Figure 12. Arc assembly.

As can be seen in Figure 12, all nonwelded seals confining the seeded gas are surrounded by cover gas. The cover gas is sealed against atmosphere by stainless steel O-rings at the flanges; by gaskets at the quartz window; by the 0.25-in. tube fitting; and the 0.375-in. tube fitting. The solid vacuum flange is also welded to the tube fitting. The other tube fitting serves as a seal between cover gas and seeded gas.

The whole assembly is wire-heated and insulated to keep all walls in contact with the seeded gas at a temperature higher than the seeding temperature to prevent condensation.

Figure 13 shows a schematic of the complete system. The gas flows from a chamber (a) through the seeding unit (b) and enters the arc chamber through the nozzle surrounding the cathode (c) and exhausts through the anode (d) into another chamber (e). From this chamber (e), the gas is pumped back into the first chamber (a) by a pump (f). The flow is directed by two check valves (g) and (h).

As a pump, a stainless steel bellows with 40 cm^2 cross section that can be compressed about 1 cm is used. This arrangement yields 40 cm^3 displacement per stroke. The bottom of the bellows is turned inside to provide higher over- and underpressure to activate the ball check valves. The chambers (a) and (e) are stainless steel cylinders (175 $\times$ 8.5 cm) with 10-liter volume. They serve as settling chambers for the gas and as evaporators and condensers for the Cs. In addition, they allow blowdown operation in case short-time, high-velocity gas flows are wanted. In this case, the pressure difference between the chambers (a) and (e) can be increased above the pressure difference attained by the pump (f) by heating one cylinder (e) and cooling the other cylinder (a) during pumping and then, with the valves closed, by cooling the first cylinder (e) and heating the second cylinder (a) up to seeding temperature.

The seeding unit (b) consists of two concentric stainless steel pipes, 175 cm long; the space between the pipes is filled by a coil made from four 0.25-in. stainless steel tubes wound in parallel on the inner pipe, giving 270 turns.

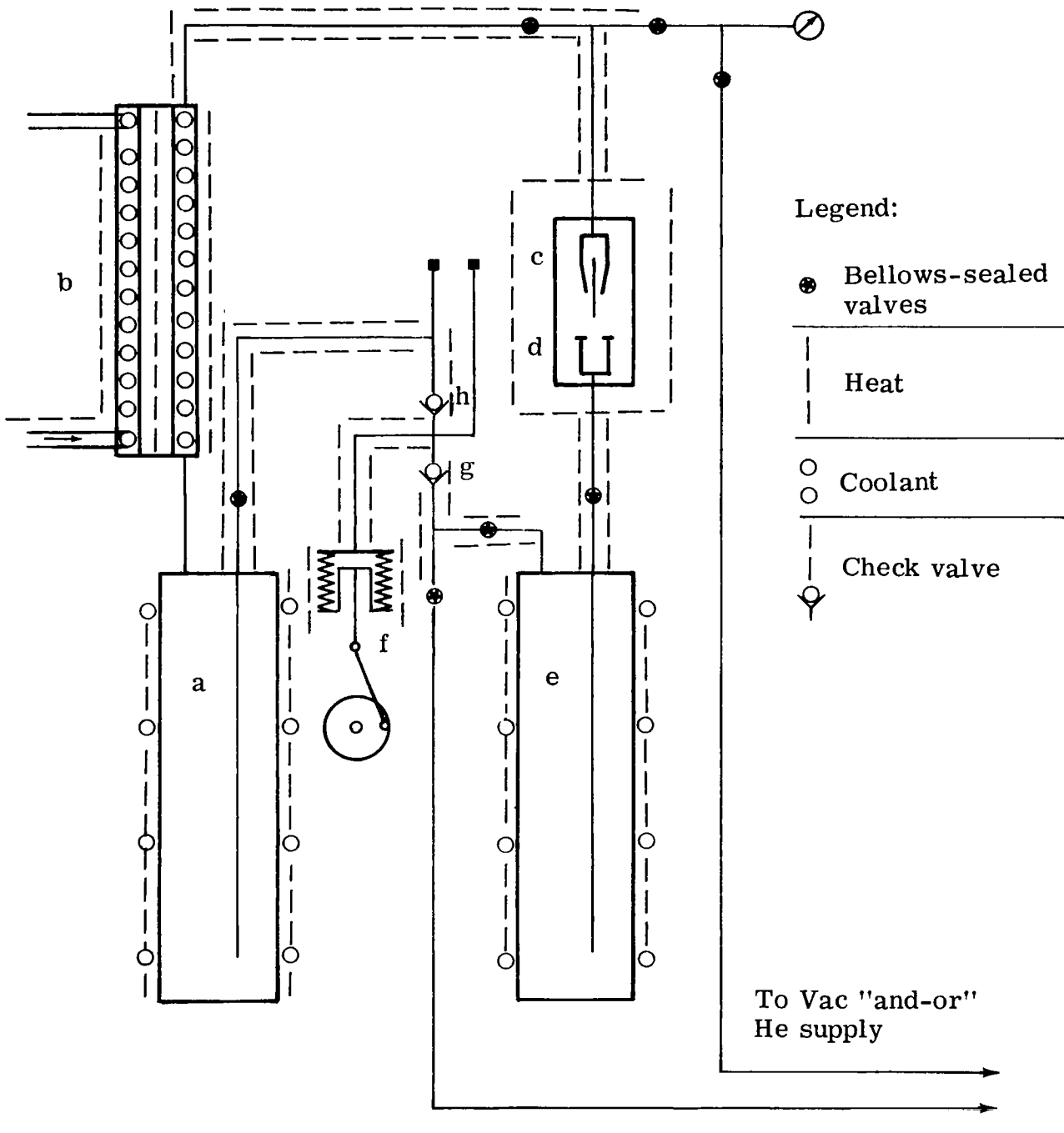

Figure 13. Schematic of system.

The cylinders (a) and (e), seeder (b), pump (f), and connecting stainless steel tubing are wrapped in Nichrome therm wire (proved up to 800°K) which would allow Cs partial pressures up to 10^2 torr. The heated parts are insulated by ceramic fiber blankets. The walls of the cylinders (a) and (e) and the seeding unit (b) are temperature controlled. Under normal operating conditions, units (a), (e), and (b) and the connecting line between (a) and (b) are kept at the selected seeding temperature, and the gas being passed through the coils of the seeding unit (b) is also preheated to seeding temperature. All other surfaces are kept at higher temperature to prevent condensation. The valves used in the system in contact with Cs are bellows-sealed stainless steel.

The system is filled with 200 gm Cs.

EXPERIMENTAL RESULTS

The Cs-seeded He arc was used to test the proposed method. The arc was imaged perpendicularly on the slit of a 10-m spectrograph. The spectrally resolved cross sections of the arc were recorded on Kodak N-1 spectrographic plates.

The atomic Cs spectrum is emitted from the region around the cathode, where the seeded He flow enters the plasma chamber. The measurements were thus restricted to a region from about 5 mm upstream to 2 mm downstream of the cathode tip.

Figure 14 shows photometric data of six Cs lines taken from the 10-amp, 65 v d-c arc with 1.2-cm electrode gap. The spectrum was taken at a cross section 1 mm in front of the cathode. The photometric measurements were made on a microdensitometer. The Cs lines were scanned in steps of 2 mm on the photometer display, corresponding to 0.13 mm along the arc diameter. The line profiles and adjacent background were recorded. The transformed densities (W) were obtained by reading the recorded transmissions on a W-scale.

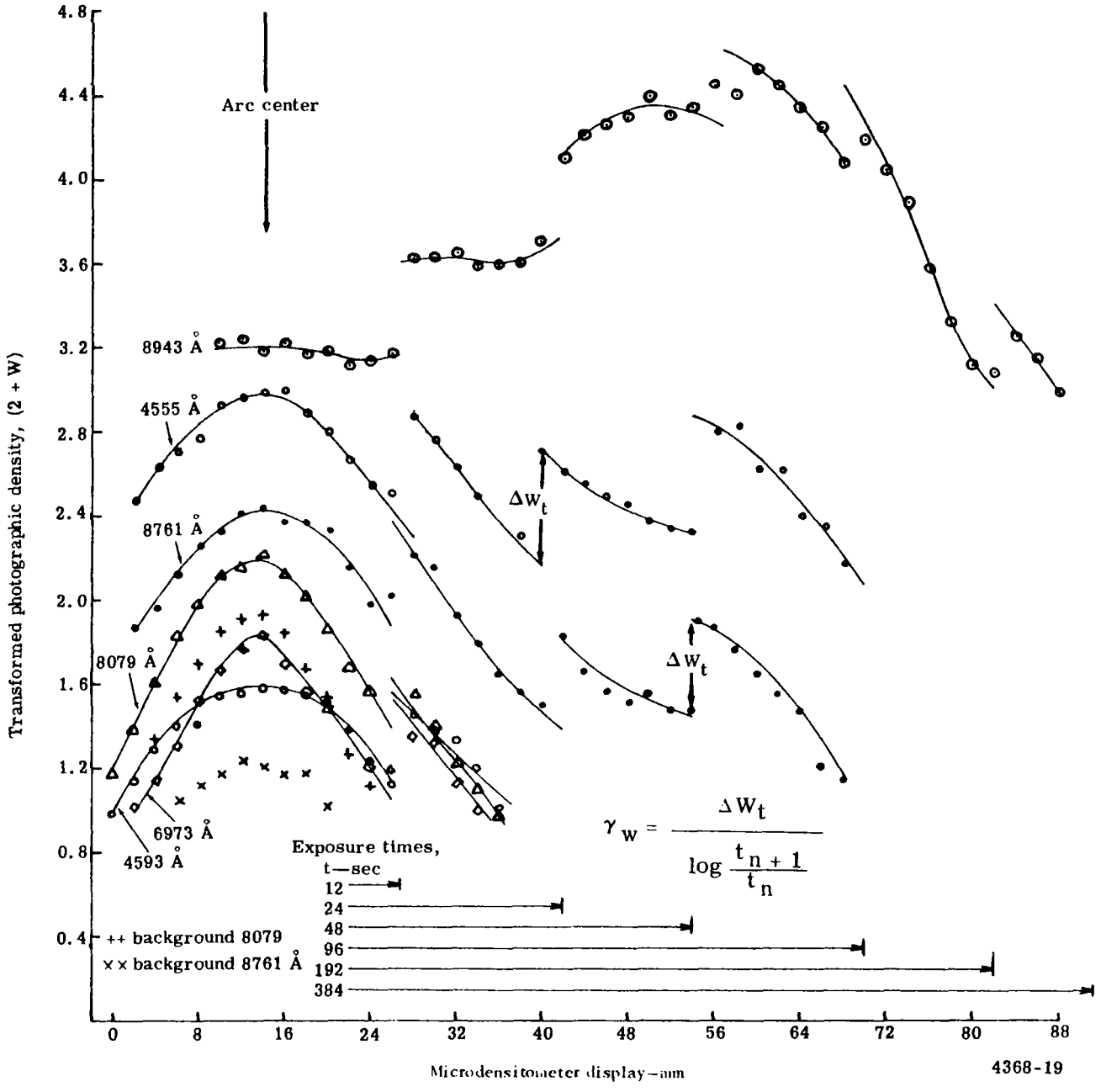

Figure 14. Photographic density profile of Cs lines versus arc diameter.

The steps ΔW_t in the W-profiles in Figure 14 represent steps of the exposure time "t" obtained by gradually shielding off the central region of the arc cross section by means of a wedge-shaped diaphragm placed in front of the spectrograph slit. Under the assumption that the reciprocity law is valid—i.e., that the photographic density is a function of the product alone (intensity × time), the γ-values for the adjacent profile sections are given by $\gamma_w = W_t/\Delta lgt$ with $\Delta lgt = lg\ 2/1 = 0.3$. From the W-plots, Figure 14, the intensity profiles are derived by subtracting the ΔW_t and dividing by the respective γ-factors. After subtracting the relatively strong background intensities from profiles $\lambda = 8761$ Å and $\lambda = 8079$ Å, three types of profiles (Figure 15) are obtained. The common quality of the profiles belonging to the same type is the upper level of the corresponding transition. Thus, the profiles of $\lambda = 8079$ and $\lambda = 6973$ are represented by λ_t with the characteristic quality $E_t = 2.6 \cdot 10^4$ cm^{-1}; $\lambda = 4555$, $\lambda = 8761$, and $\lambda = 4593$ are represented by λ_p with $E_p = 2.2 \cdot 10^4$ cm^{-1}; $\lambda = 8943$ (and $\lambda = 8521$) is represented by λ_m with $E_m = 1.1 \cdot 10^4$ cm^{-1}.

For evaluation, the profiles are converted into radial distribution by the Abels procedure (Figure 16). Since the intensity of λ_m shows an off-center peak, the temperature at point (1) can be determined by the Fowler-Milne method. Because the temperature can be assumed to rise with constant regularity toward the arc center, an off-center peak of the radial intensity corresponds to a peak of the function $I = I(T)$. In Figure 17, intensity versus temperature is plotted for the Cs lines $\lambda_m = 8943$ and $\lambda_p = 4555$, with the seeding ratio α (in atmospheric He) as parameter. With $\alpha = 10^{-8}$, I(T) for $\lambda_m = 8943$ has its maximum at 2000°K. In the present experiment, the system was kept at room temperature and the seeding ratio should be about $\alpha = 10^{-8}$. Assuming that this seeding ratio exists in point (1), the corresponding temperature would be 2000°K. The intensity, I(T), of $\lambda = 4555$ reaches a maximum at about 2100°K (Figure 17). Between 2000 and 2100°K, the intensity of $\lambda_p = 4555$ increases about 0.2 in logarithmic scale. In Figure 16, however, the intensity of λ_p increases by 1.6 between point (1) and the arc center (3) without reaching a maximum. As can be seen in Figure 17, there is no seeding ratio, α, for which $\lambda = 4555$ can increase by more than 0.4 after passing the peak temperature for $\lambda = 8943$. It has to be assumed, therefore, that α is not constant

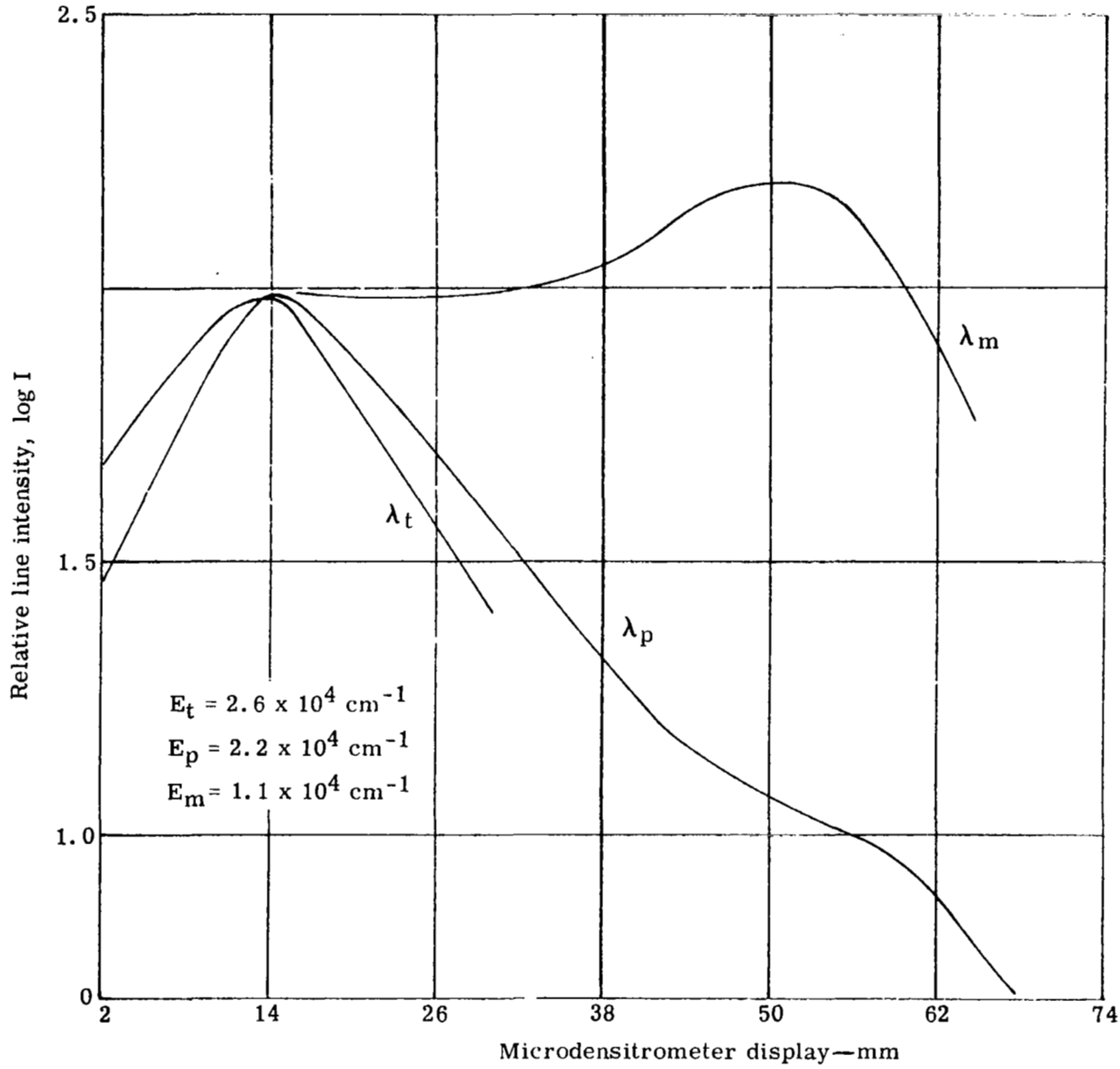

Figure 15. Observed relative line intensity distribution across arc.

throughout the cross section. In this case, the usual procedure to build up the temperature profile, starting from a known reference temperature, cannot be applied. Here a modification of the proposed method is used to determine the temperature profile and the Cs partial pressure profile. Since the quality $a = k \ln 10/E_p - E_m \cdot (\Delta Y_m - \Delta Y_p) = \frac{1}{T_1} - \frac{1}{T_2}$ does not contain the unknown pressure, it can be used to determine temperatures T_2 if a reference-temperature

T_1 is known. On the other hand, with the quality $b = \Delta Y_m + (E_m/k \ln 10) \cdot a = \lg \frac{n_o(T_1)\, u(T_2)}{n_o(T_2)\, u(T_1)} \approx \lg \frac{n_o(T_1)}{n_o(T_2)}$, the Cs partial pressure at points T_2 can be derived if the seeding ratio, a, at the point T_1 is known.

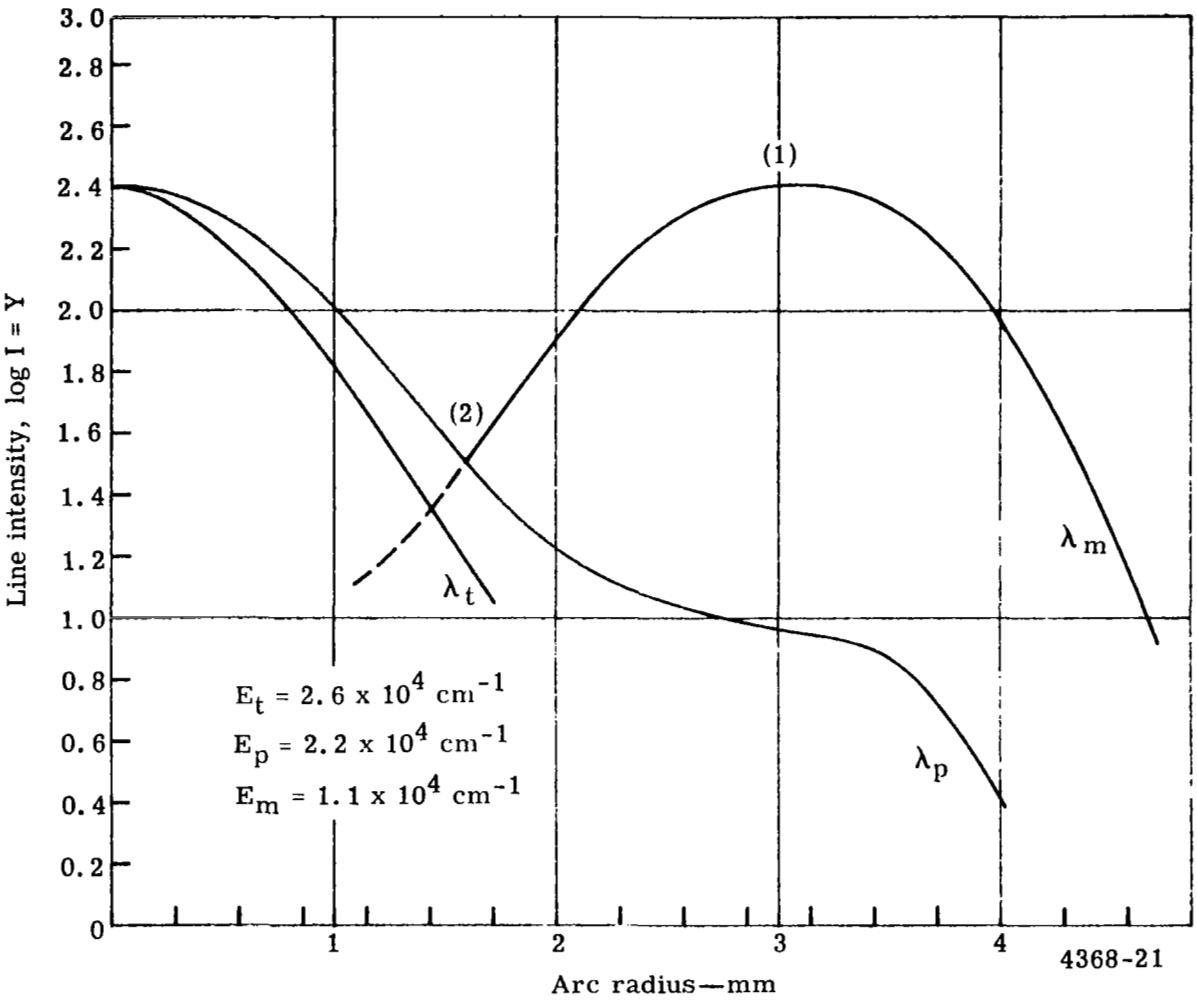

Figure 16. Relative radial intensity distribution of Cs lines with different excitation energy E (cross section 1 mm from cathode).

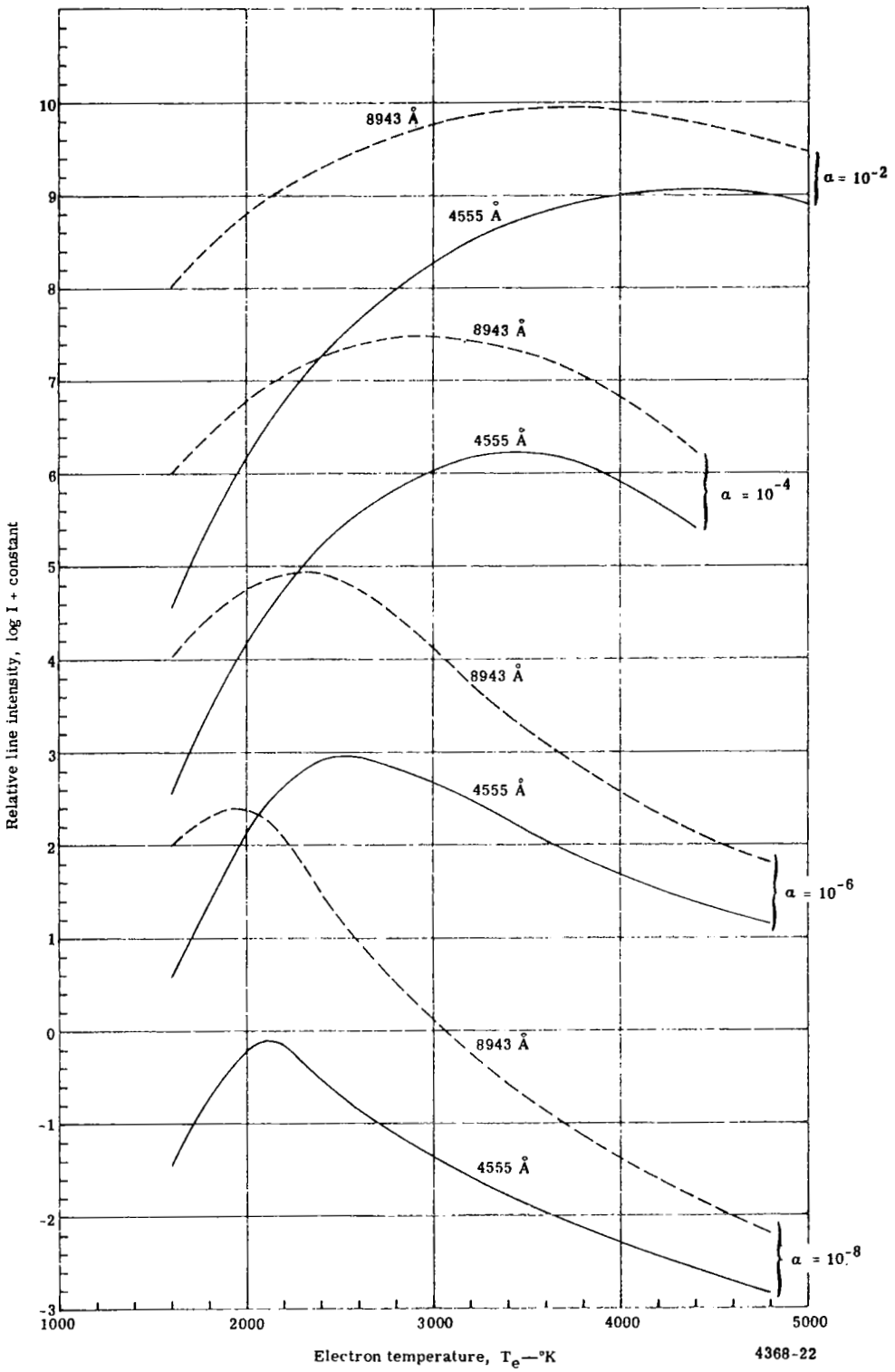

Figure 17. Theoretical log I versus T curves for Cs lines.

From Figure 16 (with log I = Y):

$Y_p(1) = 0.95$; $Y_p(2) = 1.50$; therefore,

$\Delta Y_{p_{1,2}} = Y_p(1) - Y_p(2) = -0.55$

$Y_m(1) = 2.43$; $Y_m(2) = 1.50$

$\Delta Y_{m_{1,2}} = Y_m(1) - Y_m(2) = +0.98$

From this and Equation (16): $a = \frac{k \ln 10}{E_p - E_m} \left[\Delta Y_m - \Delta Y_p\right]$ with $E_p = 2.2 \cdot 10^4$ cm^{-1}; $E_m = 1.1 \cdot 10^4$ cm^{-1}; $k \ln 10 = 1.6$ $cm^{-1}/°K$—parameter $a_{1,2} = \frac{1}{T_1} - \frac{1}{T_2}$ can be calculated $a_{1,2} = \frac{1.6}{1.1} \cdot 10^{-4} (0.90 + 0.55) = 2.11 \cdot 10^{-4}$. The b-value is calculated from the previous calculation and Equation (17):

$$b = \Delta Y_m + \frac{E_m}{k \ln 10} \cdot a;$$

$$b_{1,2} = 0.93 + \frac{1.1 \cdot 10^4}{1.6} \cdot 2.11 \cdot 10^{-4} = 2.38$$

With the calculated values $a_{1,2}$ and $b_{1,2}$, the temperature T_1 and T_2 can be determined from the parametric b-curves if the Cs partial pressure at points (1) and (2) is the same. For example, with seeding ratio $\alpha = 10^{-8}$, from Figure 10, T_1 is determined to be 1650°K; and T_2 from $1/T_2 = 1/T_1 - a = \left(\frac{1}{0.165} - 2.11\right) \cdot 10^{-4} = 3.92 \cdot 10^{-4}$; $T_2 = 2450°K$.

However, in the investigated plasma, the Cs concentration turned out to be not constant and in this case the parametric b-curves cannot be used. The measured b-values are now used to determine the relative distribution of the neutral Cs; the measured a-values yield the relative temperature distribution. Thus, if at one point in the plasma the temperature is known, the a-values give the absolute temperature profile. If at one point the number density, n_o, of the neutral Cs is known, the measured b-values give the absolute distribution of n_o. If the temperature profile is determined from the distribution

of n_o, the Cs concentration $n_o + n^+$ and the seeding ratio $n_o + n^+/n_{He}$ can be calculated with Saha's equation.

It is assumed that the Cs concentration in the outer region of the arc (i.e., point 1, Figure 16) corresponds to the seeding ratio of the stabilizing He flow (in this experiment $\alpha = 10^{-8}$, flow rate 100 cm^3/sec). Then, with $\alpha_{(1)} = 10^{-8}$, the peaking method applied on $\lambda = 8943$, gives $T_{(1)} = 2000°K$ (see Figure 17). With $T_{(1)} = 2000°K$ and $\alpha_{(1)} = 10^{-8}$, from Allison tables $n_{o\,(1)} = 1.46 \cdot 10^{10}$. Now $T_{(2)}$ and $n_{o\,(2)}$ can be calculated with the measured values $\alpha_{1,2}$ and $b_{1,2}$ from $\alpha_{1,2} = \frac{1}{T_1} - \frac{1}{T_2}$ as follows:

$$\frac{1}{T_{(2)}} = \frac{1}{T_{(1)}} - \alpha_{1,2} = \left(\frac{1}{0.2} - 2.11\right) \cdot 10^{-4} = 2.89 \cdot 10^{-4};$$

$$T_{(2)} = 3460°K \text{ from } b_{1,2} = \lg \frac{n_{o\,(1)}}{n_{o\,(2)}} \cdot \frac{u_{(2)}}{u_{(1)}},$$

$$\text{with } \frac{u_{(2)}}{u_{(1)}} \approx 1, \text{ follows } \lg n_{o\,(2)} = \lg n_{o\,(1)} - b_{1,2} =$$

$$10.16 - 2.38 = 7.78;\ n_{o\,(2)} = 6.0 \cdot 10^7$$

Temperature ($T_{(3)}$) and neutral Cs density $n_{o\,(3)}$ at the arc center (3) are calculated in the same manner.

Because the profile of λ_m is considered inaccurate in the central region due to the blanketing effect of the strong off-center maximum, profile λ_t is used instead.

From Figure 16:

$$Y_t\,(2) = 1.20;\ Y_t\,(3) = 2.40;\ Y_t\,(2) - Y_t\,(3) = \Delta Y_{t\,2,3} = 1.20$$

$$Y_p\,(2) = 1.50;\ Y_p\,(3) = 2.40;\ Y_p\,(2) - Y_p\,(3) = \Delta Y_{p\,2,3} = -0.90$$

With $E_t - E_p = 0.4 \cdot 10^{-4}$, it is:

$$a_{2,3} = \frac{k \ln 10}{E_t - E_p} (\Delta Y_{p\,2,3} - \Delta Y_{t\,2,3}) = 1.6/0.4 \cdot 10^{-4} (-0.90 + 1.20) =$$

$$1.2 \cdot 10^{-4}$$

$$b_{2,3} = \Delta Y_{p\,2,3} + E_p/k \ln 10 \cdot a_{2,3} = -0.90 + \frac{2.2 \cdot 10^4}{1.6} \cdot 1.2 \cdot 10^{-4} = 0.75$$

Now temperature and neutral Cs density at point (3) can be calculated:

$$\frac{1}{T_{(3)}} = \frac{1}{T_{(2)}} - a_{2,3} = \left(\frac{1}{0.340} - 1.20\right) \cdot 10^{-4} = 1.70 \cdot 10^4;$$

$T_{(3)} = 5900°K$ and

$$\lg n_{o\,(3)} = \lg n_{o\,(2)} = b_{2,3} = 7.78 - 0.75 = 7.03;$$

$$n_{o\,(3)} = 1.1 \cdot 10^7$$

With temperatures and neutral Cs densities known at points (2) and (3), the corresponding Cs concentration $Cs_o + Cs^+$ and seeding ratios $\frac{Cs_o + Cs^+}{He}$ are determined.

From Allison tables by interpolation:

for T (2) = 3460°K, n_o (2) = $6 \cdot 10^7$ it is α (2) = 10^{-7}

for T (3) = 5900°K, n_o (3) = $1.1 \cdot 10^7$ it is α (3) = $10^{-5.8} = 160 \cdot 10^{-8}$

The derived values for seeding ratio α and arc temperature are plotted versus arc radius in Figure 18.

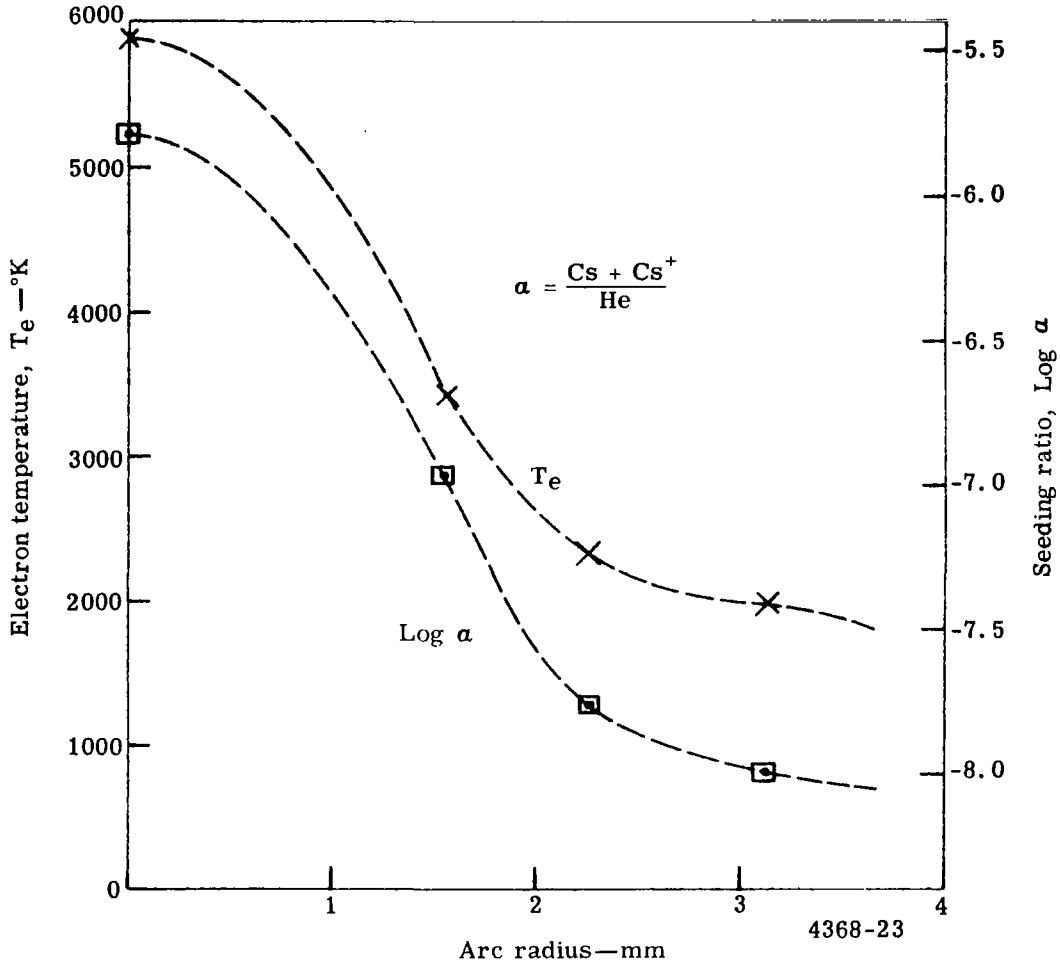

Figure 18. Temperature profile and Cs distribution at cross section 1 mm from cathode.

Allison Division of General Motors
Indianapolis, Indiana, 2 July 1965.

REFERENCES

1. Ornstein, L. S. and Brinkmann, H. in Physics 1, 797 (1934).

2. Hoermann, H. in Zeitschr. f. Physik 97, 539 (1935).

3. Maecker, H. in Zeitschr. f. Physik 136, 119 (1953).

4. Fowler, R. H. and Milne, E. A. Statistical Mechanics. Cambridge, 1936.

5. Larenz, H. in Zeitschr. f. Physik 129, 327 (1951).

6. Bartels, H. and Larenz, H. in Naturwiss. 37, 164 (1950).

7. Schneider, R. T., Wilhelm, H. E., and Woerner, W. N. Measurement of Fluid Properties for Magnetoplasmadynamic Power Generators. Allison Division, GMC, EDR 3632 (November 1963).

8. Ecker, G. and Weizel, W. in Ann. Phys. 17, 126 (1956).

9. Schneider, R. T., Wilhelm, H. E., and Woerner, W. N. Quarterly Summary Report No. 1, Spectroscopic Investigations of Plasma Properties. Allison Division, GMC, EDR 3969 (September 1964).